Exploration of Mechanisms for the Transformation of 8-Hydroxy Guanine Radical to FAPyG by Density Functional Theory

Barbara H. Munk,[†] Cynthia J. Burrows,[‡] and H. Bernhard Schlegel*[,†]

Department of Chemistry, Wayne State University, Detroit, Michigan, 48202, and Department of Chemistry, University of Utah, 315 South 1400 East, Salt Lake City, Utah 84112-0850

Received August 11, 2006

The potential energy surface for the transformation of 8-hydroxy guanine radical to formamidopyrimidine adducts via four pathways has been mapped out using B3LYP density functional theory and the IEF-polarizable continuum model (PCM) solvation model. Results of the calculations are consistent with experimental studies indicating that numerous compounds may be formed during the oxidation and subsequent reduction of guanine, some of which can react over time to form the observed 2,6-diamino-4-hydroxy-5-formamidopyrimidine (FAPyG) adduct. All four pathways begin with the 8-hydroxyguanine radical (8-OHGrad) species. Pathway 1 proceeds with reduction of the 8-OHGrad to a hemiaminal species, which undergoes ring opening to either FAPyG or 2,5-diamino-4-hydroxy-6-formamidopyrimidine (2,5FAPyG). Pathway 2 begins with a water-assisted proton transfer from the hydroxyl group of 8-OHGrad to form an 8-oxyguanine radical. This radical species can undergo ring opening and subsequent reduction to form either FAPyG or 2,5FAPyG. Pathways 3 and 4 lead to formation of only the FAPyG ring-opened adduct. Both begin with ring opening of 8-OHGrad to yield a formimidic acid radical, which can either be reduced to the formimidic acid and then undergo tautomerization to FAPyG (pathway 3) or initially tautomerize to form one of two FAPyG radicals before being reduced to FAPyG (pathway 4). Of the four possible reaction pathways explored, pathway 2 appears to be slightly lower in energy than pathway 4, which in turn is lower in energy than pathways 1 and 3. The calculations indicate that reactions proceeding via pathway 2 may yield a 2,5FAPyG adduct, which is thermodynamically less stable than the FAPyG adduct but may be formed at least initially. Interconversion of the two isomers is possible via a hemiaminal adduct. In the presence of water, it is energetically possible to form the FAPyG adduct from the formimidic acid, the hemiaminal, and the 2,5FAPyG adducts. Calculations at the B3LYP/6-31+G(d) level of theory suggest that it will be possible to differentiate between the different intermediate adducts using IR and NMR spectroscopy.

Introduction

Damage to DNA may result from exposure to reactive oxygen species created during cellular metabolism or following exposure to ionizing radiation or a variety of chemical compounds (*1*−*8*). Oxidative damage of DNA can produce nucleobase lesions, some of which are not efficiently removed by DNA's intrinsic repair mechanisms. These nucleobase lesions may produce changes in the three-dimensional structure of DNA, which can, in turn, lead to mutagenesis and contribute to aging, carcinogenesis, and neurological disease (*8*−*10*). Guanine is the most easily oxidized of the nucleobases (*1*, *11*), and this leads to the formation of two of the more prevalent DNA lesions: 8-oxo-7,8-dihydroguanine (8-oxoG)[1] (*1*, *12*−*16*) and 2,6-diamino-4-hydroxy-5-formamidopyrimidine (FAPyG) (*17*−*19*).

Several authors (*1*, *6*, *20*−*22*) note that the formamidopyrimidines [FAPyG and 4,6-diamino-5-formamidopyrimidine (FAPyA)] and 8-oxopurines (e.g, 8-oxoG) are probably produced via the same intermediate, the 8-hydroxy radical [2-amino-8-hydroxy-1,7,9-trihydropurine-6-one radical (8-OHGrad)] species (Scheme 1) with the partitioning between these pathways being dependent on the oxidizing or reducing nature of the medium (*7*). In their experimental study of the addition of hydroxyl radical to guanine, Candeias and Steenken (*4*) reported that the 8OHGrad species reacts quickly ($k = 4 \times 10^9$ m^{-1} s^{-1}) with oxygen to form 8-oxoG, but in the absence of oxygen, a rapid ($k = 2 \times 10^5$ m^{-1} s^{-1}) ring-opening reaction is observed. The authors suggest that the ring-opened species may be the N-(2,4-diamino-6-oxo-1,6-dihydropyrimidin-5-yl)formimidic acid radical (formimidic acid radical) shown in Scheme 1.

In experimental studies, several authors report that oxidation of DNA by various means leads to the formation of multiple guanine products. Arce's group (*23*) irradiated guanosine with low- and high-intensity UV light and then isolated and characterized the products using HPLC-ESI-MS and UV absorption spectroscopy. At least 14 products were created during this experiment, and release of the guanine base from the sugar was reported to be the major pathway for product formation. Upon the basis of HPLC-ESI-MS data, the authors

* To whom correspondence should be addressed. Tel: 313-577-2562. Fax: 313-577-8822. E-mail: hbs@chem.wayne.edu.

[†] Wayne State University.

[‡] University of Utah.

[1] Abbreviations: 8-OHGrad, 2-amino-8-hydroxy-1,7,9-trihydropurine-6-one radical; 8-oxoG, 8-oxo-7,8-dihydroguanine; 8-oxyG radical, 2-amino-8-oxy-1,7,8,9-tetrahydropurine-6-one radical; FAPyG, 2,6-diamino-4-hydroxy-5-formamidopyrimidine; FAPyG N7 radical, 2,6-diamino-4-hydroxy-5-formamidopyrimidine with a radical at N7 of the original purine; FAPyG N9 radical, 2,6-diamino-4-hydroxy-5-formamidopyrimidine with a radical at N9 of the original purine; formimidic acid, N-(2,4-diamino-6-oxo-1,6-dihydropyrimidin-5-yl)formimidic acid; formimidic acid radical, N-(2,4-diamino-6-oxo-1,6-dihydropyrimidin-5-yl)formimidic acid radical; hemiaminal, 2-amino-8-hydroxy-1,7,8,9-tetrahydropurine-6-one; 2,5FAPyG, 2,5-diamino-4-hydroxy-6-formamidopyrimidine; 2,5FAPyG radical, 2,5-diamino-4-hydroxy-6-formamidopyrimidine with a radical at N7 of the original purine.

10.1021/tx060187t CCC: $37.00
Published on Web 02/23/2007

Scheme 1. Literature Mechanism for the Transformation of Guanine to 8-OxoG and FAPyG[a]

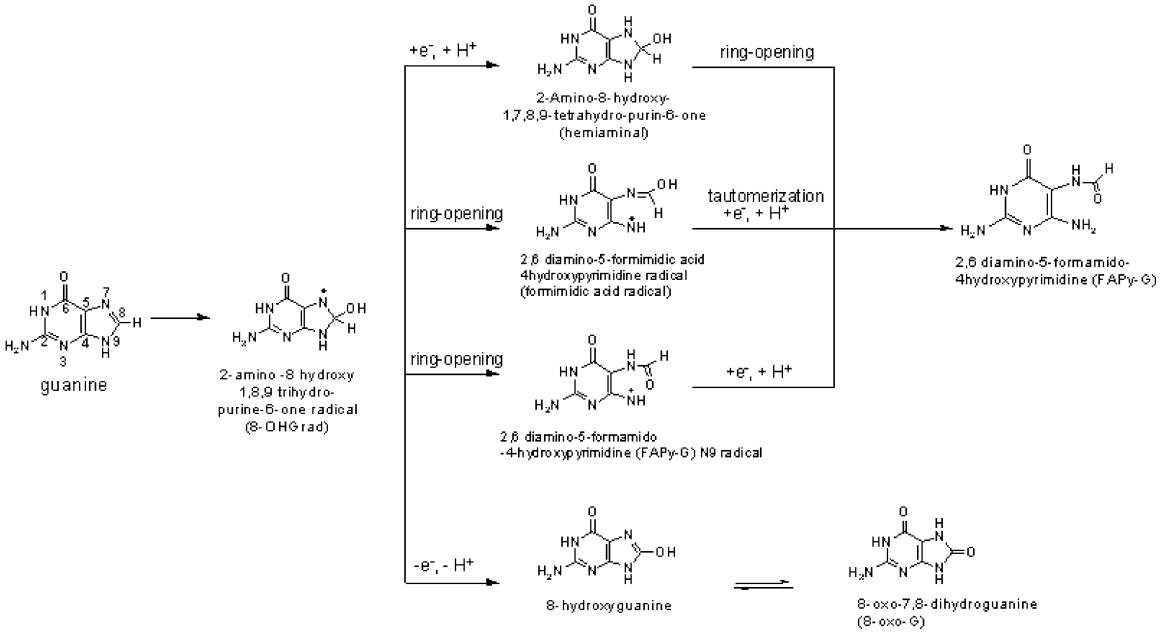

[a] Adapted from refs *1*−*8* and *26*.

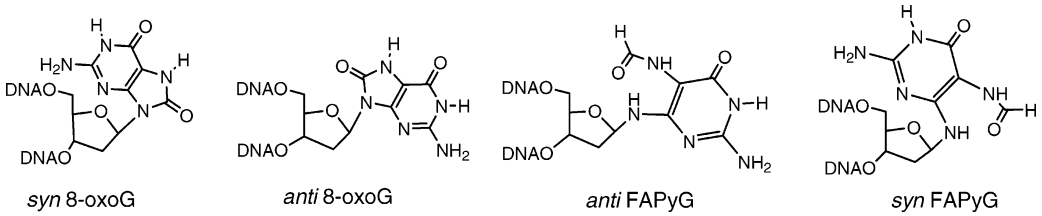

Figure 1. *Anti* and *syn* conformations of 8-oxoG and FAPyG nucleobase lesions (*24*). In double-stranded DNA, both 8-oxoG and FAPyG maintain an *anti* configuration. In single-stranded DNA, 8-oxoG rotates to the *syn* configuration.

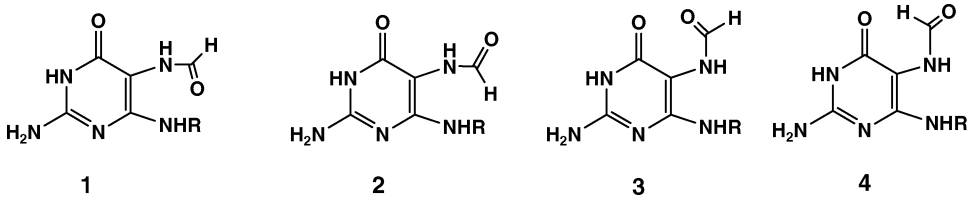

Figure 2. Rotamers of the FAPyG lesion. Two-dimensional NMR studies conducted by Burgdorf et al. (*25*) showed that only rotamers 1 and 2 are found experimentally. Structure 1 may be stabilized by an internal hydrogen bond between the formamide oxygen and the hydrogen at N9.

identified five of the 14 products as guanine and four isomers of FAPyG, which they suggest may be the α- and *β*-anomers of both the furanose and the pyranose configurations of the nucleoside. The eight other products are not identified analytically, although the authors suggest that the formamidopyrimidines are formed via a 2-amino-8-hydroxy-1,7,8,9-tetrahydropurine-6-one (hemiaminal) intermediate. Arce's results are consistent with the findings of Cadet (*17*, *18*) and van Hemmen (*19*), who observed that radiation-induced decomposition of deoxyadenosine, deoxyguanosine, or adenine resulted in the formation of a variety of products. In the case of the nucleosides, the isolated and purified formamidopyrimidine derivatives were determined by $^{1}H-^{13}C$ two-dimensional NMR experiments to be the α- and *β*-anomers of the furanose and pyranose isomers. Decomposition of adenine was found to produce six radiation products, three of which were assigned, based upon UV spectroscopy, to be the 8-oxoadenine, the ring-opened FAPyAd, and 6-amino-8-hydroxy-7,8-dihydropurine (a hemiaminal).

The conformation of monomeric FAPyG has been studied by a number of researchers. Coste et al. (*24*) reported the crystal structure of the formamidopyrimidine-DNA gylcosylase (Fpg) bound to a segment of DNA containing the FAPyG lesion. The paper also lists several DNA lesions caused by the initial oxidation of guanine including both 8-oxoG and FAPyG. The authors note that both the cis and the trans isomers of FAPyG are observed and that this lesion assumes an *anti* conformation relative to the sugar ring rather than the *syn* conformation observed with the 8-oxoguanine moiety (Figure 1).

Burgdorf and Carell (*25*) conducted experimental and computational studies on monomeric FAPyG synthesized from 2-amino-4,5-dichloropyrimidine. Temperature-dependent NMR studies conducted on the isolated compounds indicated that two different conformers existed, described as the cis and trans formamides of the 2,6-diamino-5-formamidopyrimidine (rotamers 1 and 2; Figure 2). The authors suggest that while the trans (rotamer 2) isomer should be more stable for steric reasons, the cis isomer (rotamer 1) may be observed in vivo because it is stabilized by an internal hydrogen bond between the hydrogen at N9 and the oxygen of the formamide group. Neither rotamer 3 nor rotamer 4 was observed in their NMR study. Modeling

Scheme 2. Proposed Mechanisms for the Transformation of Guanine to Two Formamidopyrimidine Isomers

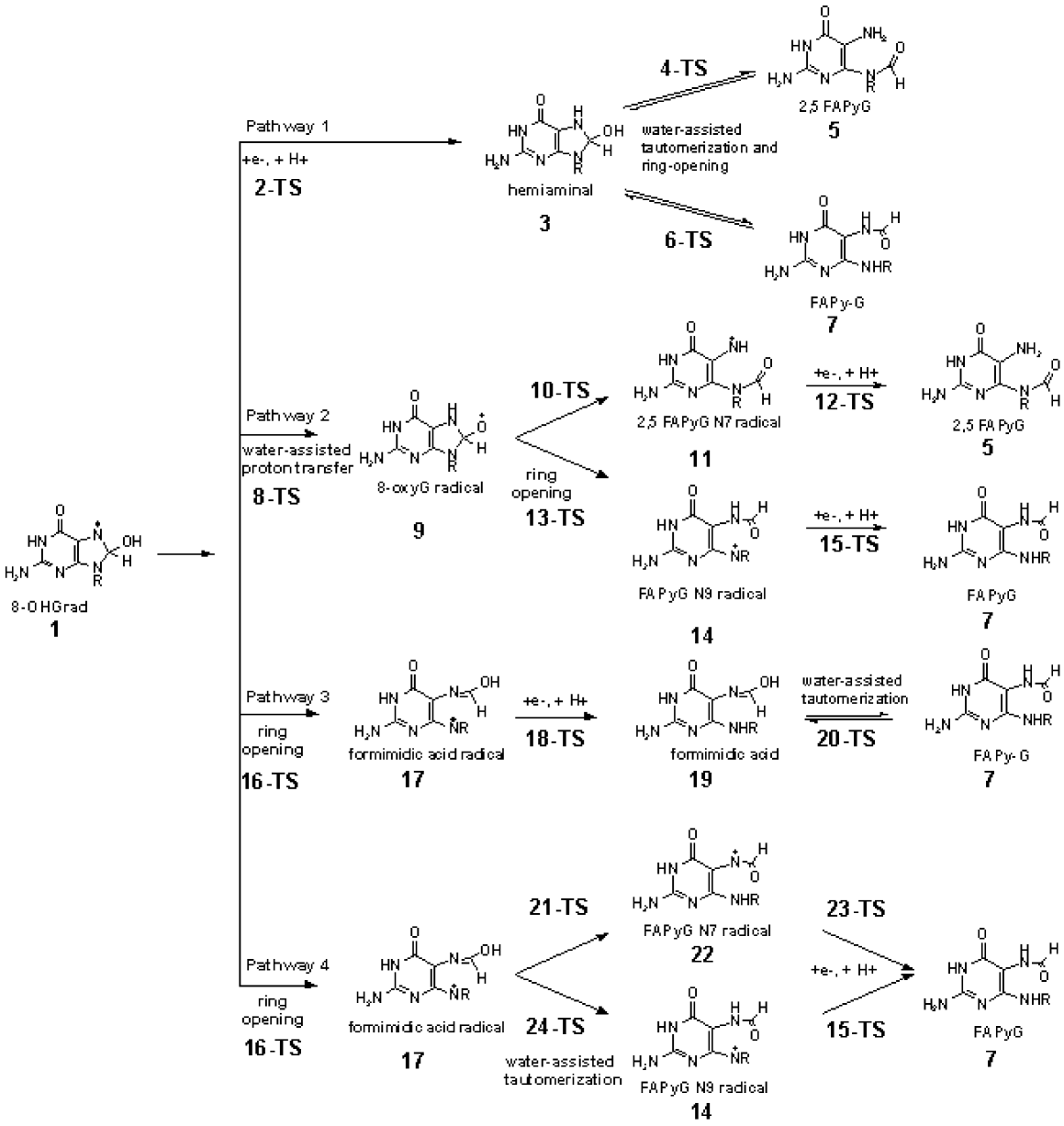

studies were conducted on four different conformers of FAPyG using force field calculations (Macromodel, MMFF94s), and these predicted that the barrier to rotation of the formamide group is about 18.5 kcal/mol. For these computations, the N9 substituent on FAPyG was hydrogen. Gas-phase calculations conducted at B3LYP/6-31+G(d) on FAPyG with hydrogen at N9 indicated that rotamer 1 was the lowest energy structure for this adduct. As a consequence, this geometry was the starting point for our gas-phase optimizations on structures substituted at N9 with hydroxymethyl and methoxyethyl groups.

Calculations on the mechanism of oxidation of guanine to 8-oxoG have been conducted by several groups. Reynisson and Steenken (*26*) have used density functional theory (DFT) to study the electrophilic addition of water to guanine and adenine radical cations to form 8-oxoguanine and 8-oxoadenine. Their calculations conducted in the gas phase at the B3LYP/6-311G-(2df,p) level of theory find that water addition to the guanine radical cation is exothermic by −75.3 kcal/mol while addition to the neutral guanine radical is endothermic by 29.4 kcal/mol. The authors suggest that these data provide an explanation for the experimental observation of 8-oxoG formation only in double-stranded DNA where the protonated radical is likely to be the predominant radical species. In a similar study, Llano and Eriksson (*27*) used DFT and a polarizable continuum model for solvation (IEF-PCM) to study two mechanisms proposed for the formation of 8-oxoG: one initiated by loss of a proton from 8-OHGrad and a second initiated by loss of a proton and electron from 8-OHGrad. At the IEF-PCM/B3LYP/6-311+G-(2df,p)//B3LYP/6-31G(d,p) level of theory, they found that the proton-coupled one-electron oxidation of 8OHGrad to 8-oxoG is energetically favored by about 12 kcal/mol. The authors also noted that the water-assisted tautomerization of 8-hydroxyguanine to 8-oxoG has a forward barrier height of 6.4 vs 38.5 kcal/mol for an unassisted proton transfer.

Jena and Mishra (*28*) used DFT, Møller−Plesset perturbation theory, PCM, and IEF-PCM to study the mechanism of formation of 8-oxoguanine following reaction of guanine with hydroxyl radical(s) and hydrogen peroxide. The forward barrier height for water-assisted tautomerization of 8-hydroxyguanine to 8-oxoG was found to be 7.0 kcal/mol at B3LYP/aug-cc-pVDZ

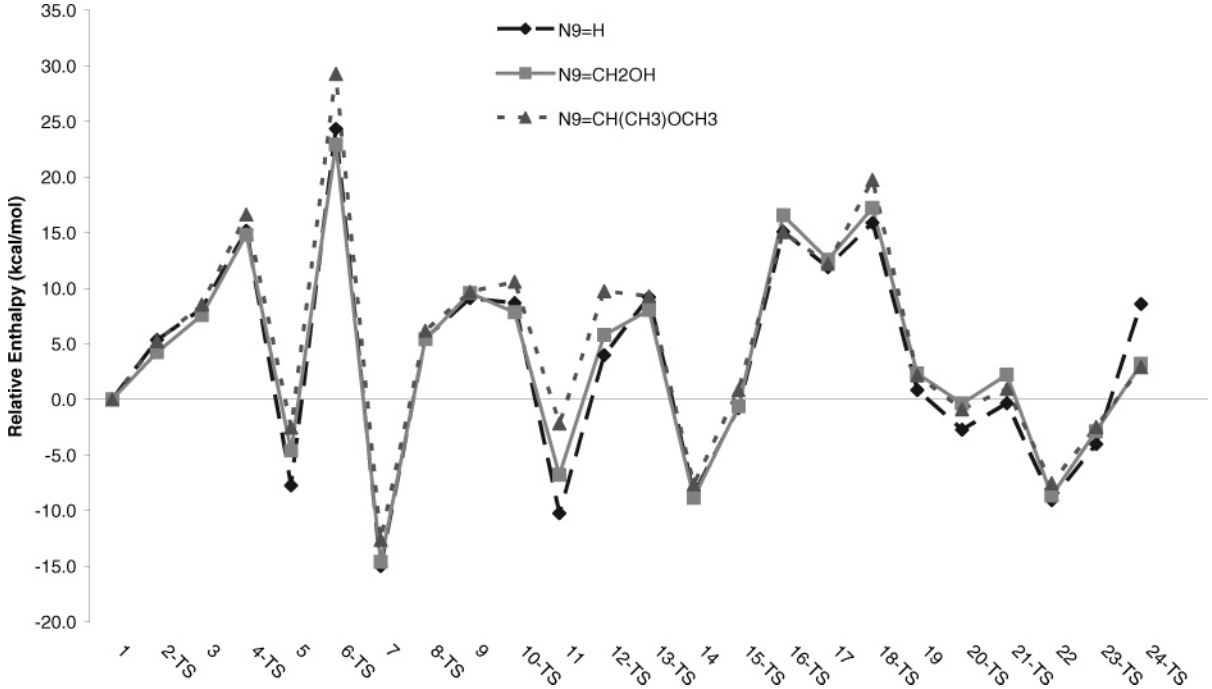

Figure 3. Comparison of the relative gas-phase enthalpy of various intermediates with substitution at N9 with H, CH_2OH, and $CH(CH_3)OCH_3$. All values are calculated at B3LYP/6-31+G(d). Descriptions of each of the intermediates and transition states are provided in Table 1. Structures for the adducts can be found in Scheme 2.

and 8.7 kcal/mol in solution at PCM/B3LYP/aug-cc-pVDZ. The formation of 8-oxoguanine from a ring-opened intermediate was found to have a higher forward barrier height and was therefore considered to be an unlikely pathway.

In the present study, we use DFT with a large basis and a PCM for solvation to evaluate open shell (radical) and closed shell mechanisms for ring opening resulting from hydroxylation of guanine at the C8 position. Our density functional calculations[2] along with the published results of others (*11*, *28*, *29*) consistently favor hydroxyl addition to C8 over C4 and C5, while experiments find C4 addition to predominate over C8 (60−70 vs 17%) (*4*, *30*, *31*). Pathways starting with C4 addition will be the subject of future calculations. In this manuscript, we explore four pathways for ring opening of 8-OHGrad (**1**), leading to FAPyG (**5**) and 2,5-diamino-4-hydroxy-6-formamidopyrimidine (2,5FAPyG, **7**) (Scheme 2). Two of these mechanisms yielding FAPyG have been examined previously by Wetmore et al. (*32*) using an unsubstituted purine and a hydrogen atom as the model compounds for the guanine nucleobase and reducing agent. Wetmore calculated the barrier for ring opening of the 8-OHGrad to a formimidic acid radical to be 24.0 kcal/mol in solution at the IEF-PCM/6-311G(2df,p)//B3LYP/6-31G(d,p) level of theory and 17.0 kcal/mol in the gas phase at B3LYP/6-31G(d,p). Using a hydrogen atom as the reducing species, Wetmore et al. suggest that the reduction of the formimidic acid radical to the closed shell species followed by tautomerization to FAPyG (pathway 3) may be favored over pathway 4, tautomerization of the formimidic acid radical followed by reduction to the FAPyG closed shell species. The water-catalyzed barrier height of the closed shell tautomerization was calculated to be 6.9 kcal/mol at the IEF-PCM/6-311G-(2df,p)//B3LYP/6-31G(d,p) level of theory. We build upon this previous research by evaluating two additional pathways, which produce 2,5FAPyG as well as FAPyG, modeling the reduction step with a thiol instead of a hydrogen atom and examining the effects of different substituents at N9 that more closely model the sugar linkage.

[2] Munk, B. H., and Schlegel, H. B. Unpublished results.

Materials and Methods

Molecular orbital calculations were carried out using the development version of the Gaussian series of programs (*33*). Optimized geometries and energies in the gas phase were computed with the B3LYP density functional method (*34*−*36*) using the 6-31+G(d) basis set (*37*−*42*). Model compounds for the calculations were the guanine nucleobase substituted at N9 with H, CH_2OH, and $CH(CH_3)OCH_3$ in place of the deoxyribose sugar. In the case of the methoxyethyl substituent, the geometry of this substituent was fixed to approximate that found in the deoxyribose sugar ring attached to guanine. The effect of the substituents on the relative energies is summarized in Figure 3. Transition states involving proton transfer from the hydroxyl group at C-8 to either the N-7 or the N9 of the imidazole ring were modeled with one explicit molecule of water assisting the proton transfer. The transition states thus formed were six-membered rather than four-membered ring systems and should therefore represent a lower energy pathway. This proton transfer was similar to the tautomerization of 8-hydroxyguanine to 8-oxoG previously reported by Llano and Eriksson (*27*) whose calculations estimated the solution-phase free energy forward and reverse barrier heights to be 41.6 and 52.6 kcal/mol for the four-membered transition state and 7.0 and 18.2 kcal/mol for the transition state with an explicit water [IEF-PCM/B3LYP/6-311+G(2df,p)//B3LYP/6-31+G(d,p)]. Our gas-phase calculations for the tautomerization of 8-hydroxyguanine to 8-oxoG at the B3LYP/6-31G(d) level of theory indicated that the forward and reverse enthalpic barrier heights were 38.5 and 53.4 kcal/mol for the nonassisted proton transfer and 6.4 and 16.0 kcal/mol for the water-assisted transfer. A comparison of the geometries of the two transition states is provided in Figure 4a.

Single-point calculations in aqueous solution were carried out at the gas-phase-optimized geometry for the methoxyethyl-substituted adducts and corresponding transition states using the integral equation formalism of the PCM (IEF-PCM) (*43*−*48*) at the B3LYP/aug-cc-pVTZ (*49*) level of theory. The computations were conducted with the E05 development version of the Gaussian

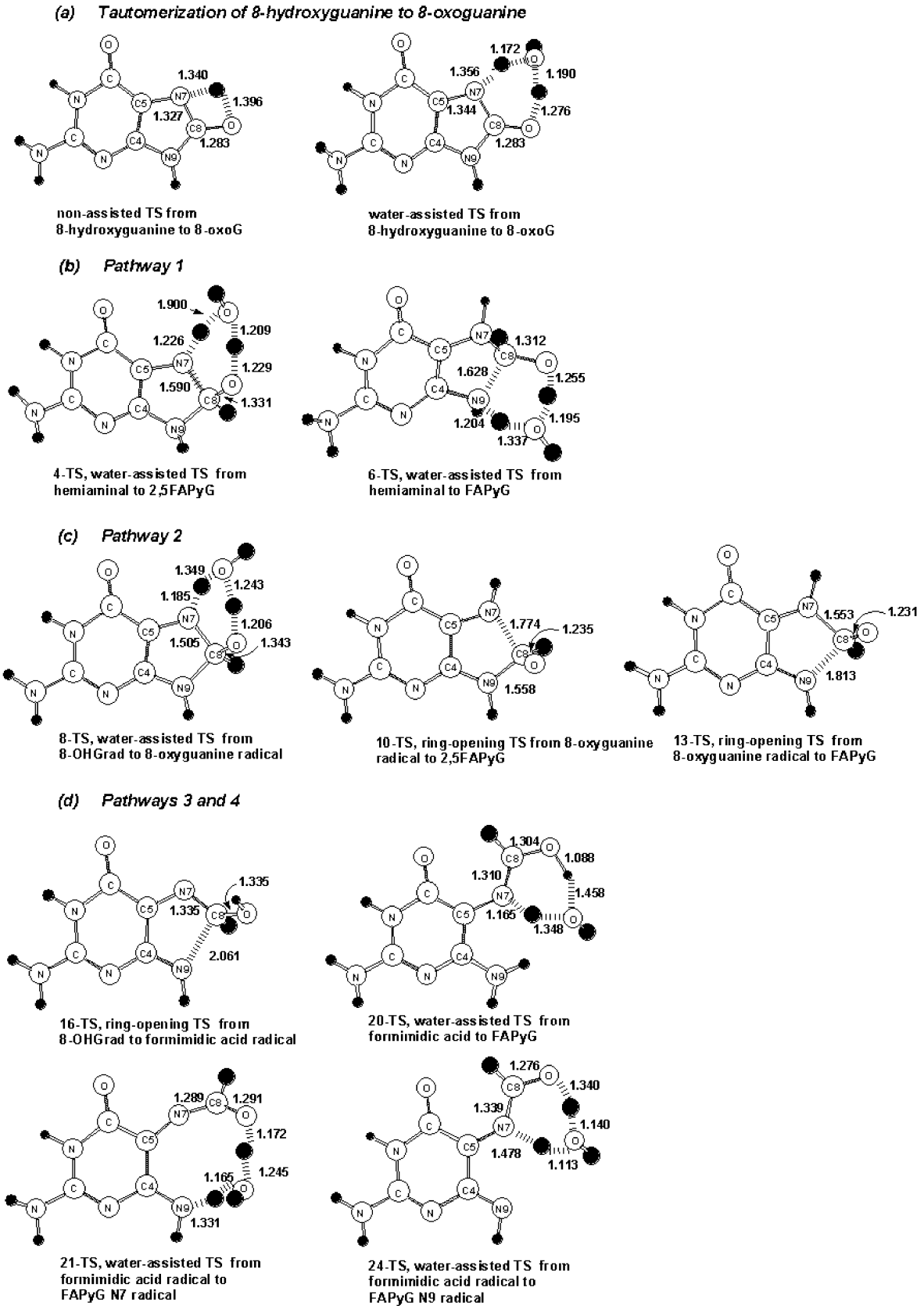

Figure 4. Transition-state geometries calculated in the gas phase at B3LYP/6-31+G(d) for adducts with hydrogen as the N9 substituent. Hydrogen atoms are indicated by filled black circles. Nonhydrogen atoms are numbered relative to their original position in the guanine nucleobase.

suite of programs and employed a solvent-excluding surface cavity model and tesserae with an average area of 0.200 Å^2. The geometries optimized in the gas phase at B3LYP/6-31G(d) for the adducts and transition states are provided in the Supporting Information. Selected optimized geometries are shown in Figures 4 and 5. Calculations for the relative energy of electron and proton transfer with oxidized guanine were conducted using methane thiol. This compound was selected as the smallest possible model for dithiothreitol, a reagent commonly used experimentally for examining electron and proton transfer within DNA. In a previous study

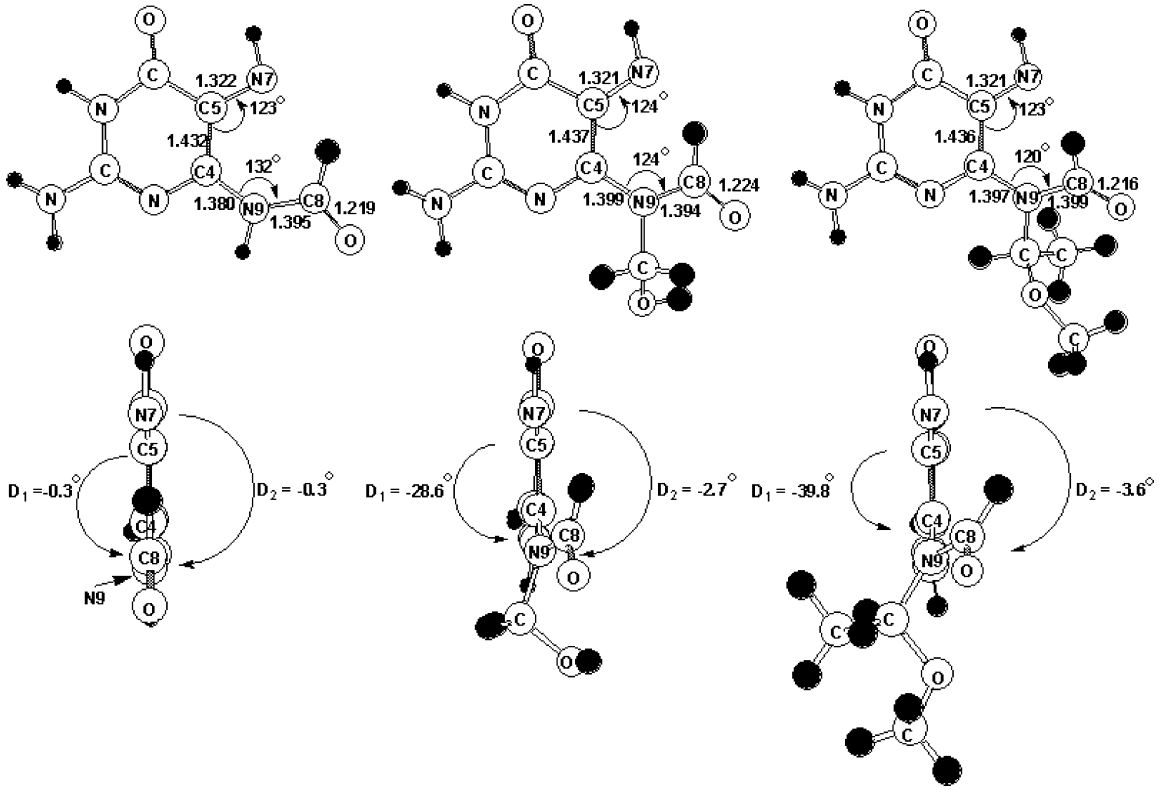

Figure 5. Influence of the N9 substituent on the geometry of the 2,5FAPyG radical, **11**. Hydrogen atoms are indicated by filled black circles. Nonhydrogen atoms are numbered relative to their original position in the guanine nucleobase. D_1 is the dihedral angle between C5 and C8; D_2 is the dihedral angle between N7 and N9.

conducted by Oikawa (*50*), thiols were shown to play a role in the oxidative damage of DNA. Dithiothreitol ($pK_a = 9.2-10.1$) (*51*) is commonly used as an in vitro reducing agent in place of the physiological thiols, such as dihydrolipoic acid ($pK_a = 4.9$ for acid group, 10.7 for thiol) and mercaptopyruvate. Pre- and post-transition state complexes with water, methane thiol, or methane thiol radical were calculated in the gas phase where appropriate. Energy profiles for pathways 1−4 are provided in Figures 6−9.

Vibrational frequencies were computed at the B3LYP level with the 6-31+G(d) basis set and were used without scaling since the B3LYP frequencies agree quite well with experimental values for a wide range of second and third period compounds (*52*). Thermal corrections and enthalpies were calculated by standard statistical thermodynamic methods (*53*) using the unscaled B3LYP frequencies and the ideal gas/rigid rotor/harmonic oscillator approximations. Infrared spectra for the 2,5FAPyG (**5**), FAPyG (**7**), hemiaminal (**3**), and formimidic acid [N-(2,4-diamino-6-oxo-1,6-dihydropyrimidin-5-yl)formimidic acid, **19**] compounds were generated using GaussView and Excel from calculated gas-phase frequency and intensity data. A graphical representation of the IR data is provided in Figure 10. NMR shielding tensors were also calculated on several geometry-optimized structures in the gas phase using Gauge Including/Invariant Atomic Orbitals (GIAO) and the B3LYP level of theory, a method shown to have a mean absolute deviation between experimental and predicted chemical shifts of approximately 10 ppm for ^{13}C NMR and 20 ppm for ^{15}N NMR (*54*−*56*).

Results and Discussion

As noted previously, several research groups have explored the possible mechanisms for formation of 8-OHGrad (**1**) from guanine (*1*, *2*, *4*, *26*, *27*, *29*, *32*, *57*). The transformation of the 8-OHGrad adduct into the biologically relevant formamidopyrimidine, FAPyG, is the focus of this research.

Gas-Phase Calculations. The relative enthalpies in the gas phase are provided in Table A of the Supporting Information and were calculated at B3LYP/6-31+G(d) for guanine substituted at N9 with hydrogen, hydroxymethyl, and methoxyethyl groups. These calculations examine the effect of the size of the N9 substituent on the potential energy surface and extend the work of previous researchers who have conducted their calculations using either a hydrogen or a methyl group at the N9 of the model nucleobase (*25*−*28*, *32*). Figure 3 maps the gas-phase energies of various adducts with different substituents at the N9 position of guanine. With the exception of 2,5FAPyG (**5**), its N7 radical (**11**), and the corresponding transition state (**12**-TS), the calculated relative enthalpies of the various intermediates are within a few kcal/mol of each other and consequently yield similar energy profiles to those observed with hydrogen as the substituent at N9. The shift in the enthalpy of the 2,5FAPyG species relative to 8-OHGrad appears to be due to the steric bulk of the N9 substituent. As shown in Figure 5, the C4−N9−C8 angle of the 2,5-diamino-4-hydroxy-6-formamidopyrimidine with a radical at N7 of the original purine (2,5FAPyG radical) decreases as the N9 substituent increases in size from hydrogen to hydroxymethyl to the methoxyethyl group. As the size of the substituent increases, the magnitude of the out-of-plane twist of the formamide group also increases from −0.3 to −39.8°, thus decreasing the stabilization energy provided by delocalization of the carbonyl electron pair. Decreased delocalization is supported by the approximately 0.02 Å increase in the length of the C4−N9 bond length between the hydrogen and the methoxyethyl substituents. For the hydrogen substituent in the gas phase at the B3LYP/6-31+G(d) level of theory, 2,5FAPyG radical is 1.7 kcal/mol more stable than the 2,6-diamino-4-hydroxy-5-formamidopyrimidine with a radical at N9 of the original purine (FAPyG N9 radical). In the case of the hydroxymethyl and methoxyethyl substituents, the FAPyG N9 radical is more stable by 2.0 and 5.4 kcal/mol, respectively.

Table 1. Relative Energies in Solution of Reactions of N9-Methoxyethylguanine[a]

summary of energetics	Scheme 2 structure no.	E + ZPE + ΔG_{solv} (kcal/mol) N9 = $CH(CH_3)OCH_3$
guanine + $^{\bullet}OH$ + H_2O + CH_3SH		29.6
8-OHGrad + H_2O + CH_3SH	**1**	0.0
8-OHGrad·CH_3SH TS + H_2O	**2**-TS	13.0
hemiaminal + H_2O + CH_3S'	**3**	11.3
hemiaminal ring opening TS to 2,5FAPyG isomer + $CH_3S^{\bullet}$	**4**-TS	31.3
2,5FAPyG + H_2O + $CH_3S^{\bullet}$	**5**	7.8,[b] 8.7[c]
hemiaminal ring opening TS to FAPyG + $CH_3S^{\bullet}$	**6**-TS	45.2
FAPyG + H_2O + $CH_3S^{\bullet}$	**7**	−3.3,[b] 0.8[c]
8-OHGrad·H_2O TS + CH_3SH	**8**-TS	18.6
8-oxyGrad + H_2O + CH_3SH	**9**	8.0
8-oxyGrad ring opening TS to 2,5FAPyG radical + CH_3SH	**10**-TS	11.5
2,5FAPyG radical + H_2O + CH_3SH	**11**	4.7
2,5FAPyG radical·CH_3SH TS + H_2O	**12**-TS	18.9
8-oxyGrad ring opening TS to FAPyG N9 radical + CH_3SH	**13**-TS	8.7
FAPyG N9 radical + H_2O + CH_3SH	**14**	0.6
FAPyG N9 radical·CH_3SH TS + H_2O	**15**-TS	11.1
8-OHGrad TS to formimidic acid radical	**16**-TS	19.5
formimidic acid radical + H_2O + CH_3SH	**17**	14.1
formimidic acid radical·CH_3SH TS + H_2O	**18**-TS	28.3
formimidic acid + $CH_3S^{\bullet}$ + H_2O	**19**	5.5
formimidic acid H_2O-assisted TS to FAPyG +$CH_3S^{\bullet}$	**20**-TS	18.9
formimidic acid radical·H_2O TS to FAPyG N7 radical + CH_3SH	**21**-TS	19.7
FAPyG N7 radical + H_2O + CH_3SH	**22**	−1.6
FAPyG N7 radical·CH_3SH TS + H_2O	**23**-TS	8.2
formimidic acid radical·H_2O TS to FAPyG N9 radical + CH_3SH	**24**-TS	22.5

[a] Solution-phase data were conducted at IEF-PCM/B3LYP/aug-cc-pVTZ//B3LYP/6-31+G(d) and include the single-point electronic energies with B3LYP/6-31+G(d) zero-point corrections. [b] These data are for the *anti* conformation. [c] These data are for the *syn* conformation.

Solution-Phase Calculations. In light of the gas-phase results summarized above, the solution-phase calculations were only carried out with the methoxyethyl substituted adducts. Table 1 lists the relative energy in solution of the reactants, intermediates, products, and transition states for the formation of two FAPyG isomers. Figure 4 provides the structures and important features of several key transition states. Figures 6−9 provide solution-phase energy profiles for the closed shell pathways and the open shell or radical pathways, with a methoxyethyl group at N9.

Closed Shell Mechanism for Formation of FAPyG Isomers (Pathway 1). Scheme 2 outlines the reaction pathways for both the closed shell and the open shell (radical) mechanisms. Pathway 1, the closed shell pathway, begins with reduction of the 8-OHGrad (**1**) to the hemiaminal (**3**). The hemiaminal adduct then undergoes ring opening to yield either FAPyG (**7**) or 2,5FAPyG (**5**).

Using CH_3SH as a model for the reducing agent, reduction of 8-OHGrad to the hemiaminal is estimated to be endothermic by 11.3 kcal/mol and is predicted to have a forward barrier height of 13.0 kcal/mol (Table 1 and Figure 6). The imidazole ring of the hemiaminal could open to form either the 2,5FAPyG or the FAPyG isomer. Both pathways are exothermic, with changes in relative energy estimated to be 3.5 kcal/mol for the 2,5FAPyG isomer and 14.6 kcal/mol for FAPyG. The transition state for this proton shuttle and ring-opening process involves an explicit molecule of water as shown in Figure 4b. At the IEF-PCM/B3LYP/aug-cc-pVTZ//B3LYP/6-31+G(d) level of theory, forward barrier heights for conversion of the hemiaminal to 2,5FAPyG (**4**-TS; Figure 4b) and FAPyG (**6**-TS; Figure 4b) are 20.0 and 33.9 kcal/mol, respectively, suggesting that 2,5FAPyG is the kinetically preferred isomer via this pathway. FAPyG is estimated to be 8.1−11.1 kcal/mol more stable than the 2,5FAPyG isomer depending on whether it is in the *syn* or *anti* configuration and would therefore be the thermodynamically preferred isomer.

Open Shell (Radical) Mechanisms for Formation of FAPyG Isomers. As shown in Figures 6−9 and Scheme 2, there are three radical mechanisms that yield FAPyG, one of which yields both the FAPyG and the 2,5FAPyG isomer. Pathway 2 proceeds via the 8-oxyguanine radical intermediate [2-amino-8-oxy-1,7,8,9-tetrahydropurine-6-one radical (8-oxyG radical, **9**)] and pathways 3 and 4 via the formimidic acid radical (**17**). Pathways 3 and 4 differ in the timing of the reduction step. As with the closed shell mechanism, pathway 2 can lead to either ring-opened isomer while pathways 3 and 4 yield only FAPyG. Table 1 provides a summary of the relative energies calculated at the IEF-PCM/B3LYP/aug-cc-pVTZ//B3LYP/6-31+G(d) level of theory.

Pathway 2. Water-assisted proton transfer from the hydroxyl group of 8-OHGrad to N7 (**8**-TS; Figure 4c) is estimated to be endothermic by 8.0 kcal/mol. This reaction leads to the formation of the 8-oxyG radical (Scheme 2 and Figure 7). Solution-phase calculations with one molecule of water indicate that the forward barrier height for this reaction is 18.6 kcal/mol. The 8-oxyG radical can undergo ring opening (**10**-TS and **13**-TS; Figure 4c) to form either the FAPyG N9 radical (**14**) or the 2,5FAPyG radical (**11**). The barrier for this ring-opening step appears to be small for both the 2,5FAPyG radical (3.5 kcal/mol) and the FAPyG N9 radical (0.7 kcal/mol). Interconversion of the two radical species via the 8oxyG radical seems feasible given that the reverse barrier height is calculated to be 6.8 kcal/mol for the 2,5FAPyG radical and 8.1 kcal/mol for the FAPyG N9 radical.

The solution-phase calculations indicate that reduction of the 2,5FAPyG radical by methane thiol is endothermic by 3.1 kcal/mol (Table 1). Reduction of the FAPyG N9 radical is predicted to be exothermic by 3.9 kcal/mol. Using CH_3SH as a model for the reducing agent, the solution phase forward barrier height for this reaction is estimated to be 14.2 kcal/mol for the 2,5FAPyG isomer. At the same level of theory, the forward barrier height for reduction of the FAPyG N9 radical is predicted to be lower, at 10.5 kcal/mol. These data suggest that the FAPyG isomer may be preferred kinetically if the reaction proceeds via pathway 2.

Pathway 3. Ring opening of 8-OHGrad to the formimidic acid radical species (**16**-TS; Figure 4d), pathway 3 (Scheme 2 and Figure 8), is endothermic by 14.1 kcal/mol. In aqueous solution, reduction of the formimidic acid radical species to yield formimidic acid (**19**) is expected to be moderately exothermic (8.6 kcal/mol). Using CH_3SH as a model for the reducing agent, the forward barrier height for this reaction is expected to be 14.2 kcal/mol. Following reduction, the formimidic acid can tautomerize to form FAPyG (**20**-TS; Figure 4d). The solution-phase tautomerization is estimated to be exothermic by 8.8 kcal/mol. The calculated forward barrier height for this water-assisted transition is 13.4 kcal/mol at the IEF-PCM/B3LYP/aug-cc-pVTZ//B3LYP/6-31+G(d) level of theory.

Pathway 4. The first step along pathway 4 (Scheme 2 and Figure 9) is the same as that discussed previously for pathway 3, endothermic ring opening of 8OHGrad to the formimidic acid radical species. Water-assisted tautomerization of this radical

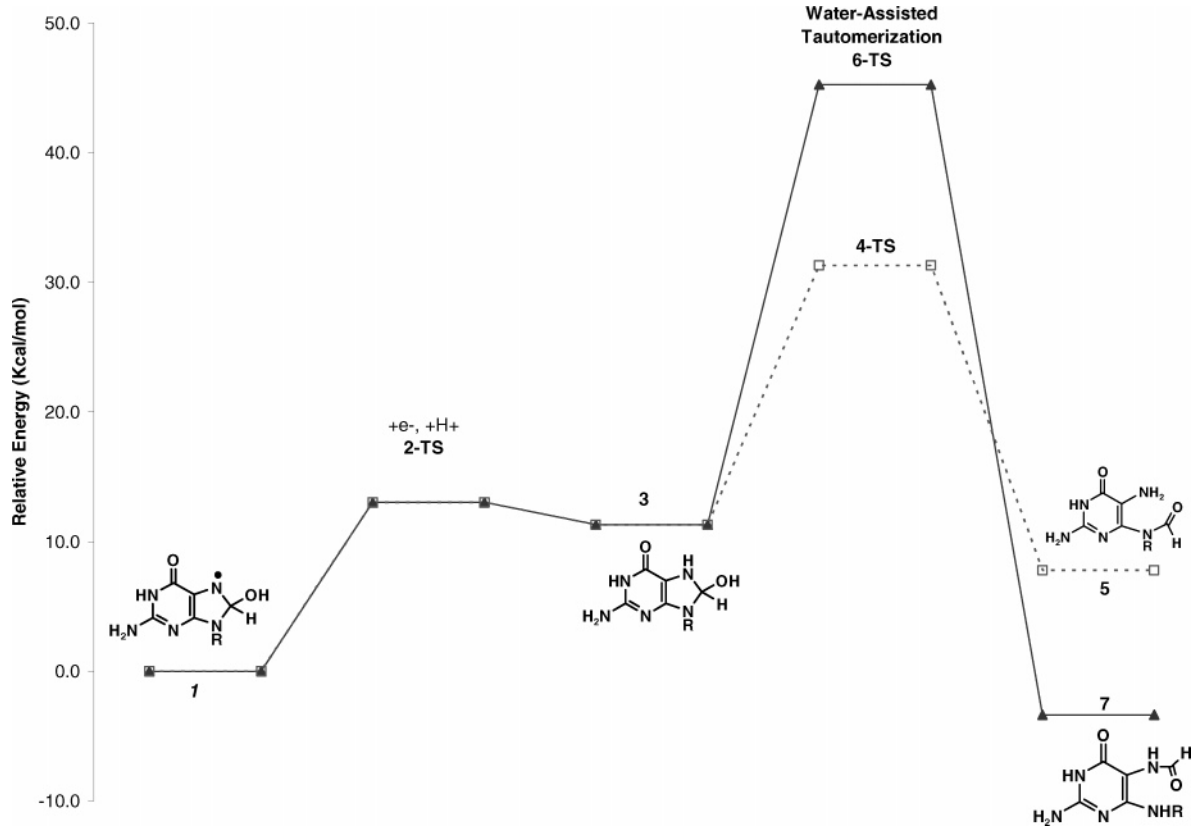

Figure 6. Pathway 1: Relative energy in solution of the closed shell mechanism for the ring opening of 8-OHGrad (**1**) to the 2,5FAPyG (**5**) and FAPyG (**7**) isomers via the hemiaminal (**3**) calculated at IEF-PCM/B3LYP/aug-cc-pVTZ//B3LYP/6-31G(d). The data are for the adducts with methoxyethyl as the N9 substituent. Ring opening of the hemiaminal has a forward barrier height of 20.0 kcal/mol for 2,5FAPyG and 33.9 kcal/mol for FAPyG.

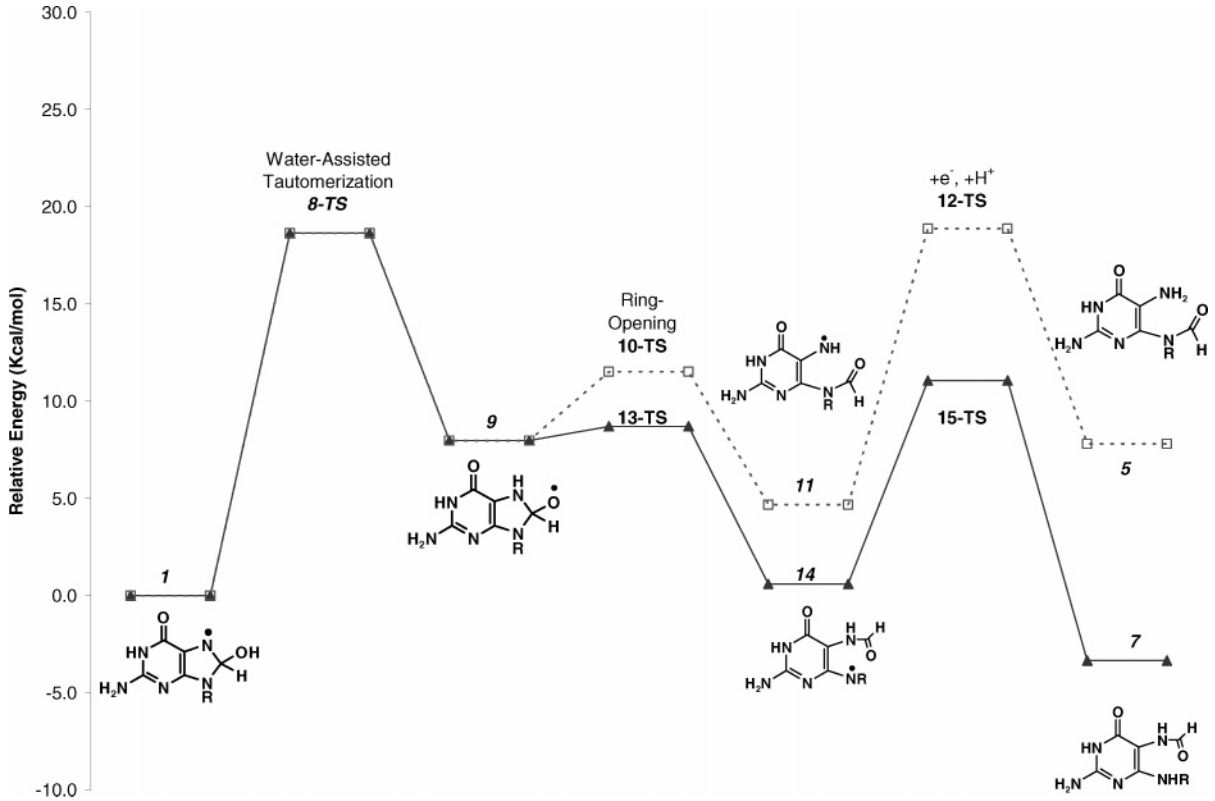

Figure 7. Pathway 2: Relative energy in solution of the open shell (radical) mechanism for the ring opening of 8-OHGrad (**1**) to 2,5FAPyG (**5**) and FAPyG (**7**) isomers via the 8-oxyG radical (**9**) calculated at IEF-PCM/B3LYP/aug-cc-pVTZ//B3LYP/6-31G(d). The data are for the adducts with methoxyethyl as the N9 substituent. Water-assisted proton transfer between the 8-OHGrad and the 8-oxyG radical has a forward barrier height of 18.6 kcal/mol. Ring opening of the 8-oxyG radical is 3.5 kcal/mol for the 2,5FAPyG radical and 0.7 kcal/mol for the FAPyG radical.

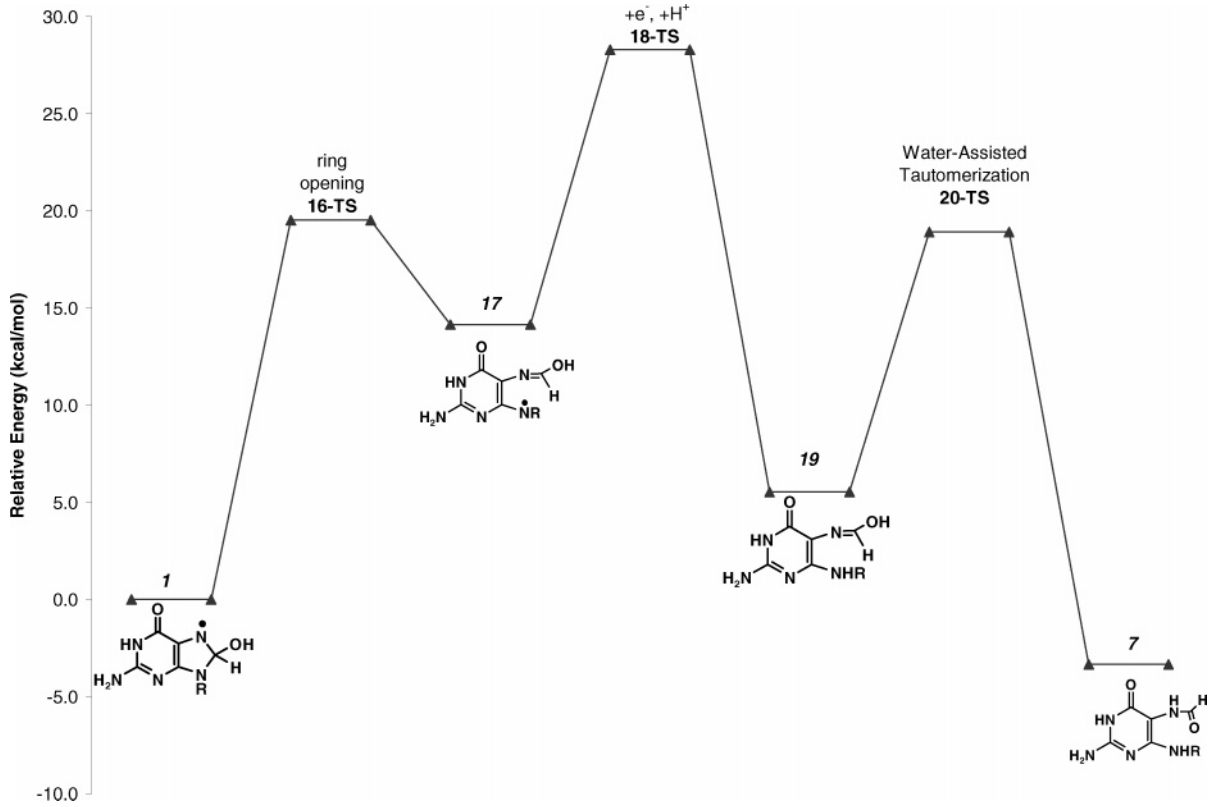

Figure 8. Pathway 3: Relative energy in solution of the open shell (radical) mechanism for the ring opening of 8-OHGrad (**1**) to FAPyG (**7**) via the formimidic acid adduct (**19**) calculated at IEF-PCM/B3LYP/aug-cc-pVTZ//B3LYP/6-31G(d). The data are for the adducts with methoxyethyl as the N9 substituent. The forward barrier height for ring opening of the 8-OHGrad to the formimidic acid radical is calculated to be 19.5 kcal/mol. Water-assisted tautomerization of the formimidic acid moiety has a forward barrier height of 13.4 kcal/mol.

species leads to either the FAPyG N7 (**22**) or the FAPyG N9 (**14**) radical. In solution at the IEF-PCM/B3LYP/aug-cc-pVTZ//B3LYP/6-31+G(d) level of theory, the forward barrier heights for formation of the N7 radical and N9 radicals are estimated to be 5.6 and 8.4 kcal/mol, respectively. Reduction of the two radical species to FAPyG is predicted to be exothermic by 1.7 kcal/mol for the N7 radical and 3.9 kcal/mol for the N9 radical. The forward barrier height for reduction of the N7 radical is estimated to be about 0.7 kcal/mol lower than that for reduction of the N9 radical. The data suggest that the preferred route for pathway 4 may be via the 2,6-diamino-4-hydroxy-5-formamidopyrimidine with a radical at N7 of the original purine (FAPyG N7 radical).

The energetics of pathways 3 and 4 have been previously explored by Wetmore et al. (*32*) at the IEF-PCM/B3LYP/6-311G(2df,p)//B3LYP/6-31G(d,p) level of theory using purine as the model for the nucleobase instead of the N-9-substituted guanine and hydrogen rather than methane thiol as the model-reducing agent. Because they used the hydrogen atom as the reducing agent, Wetmore et al. find that pathway 3, reduction of the formimidic acid radical to the closed shell species followed by tautomerization to FAPyG, may be slightly preferred over pathway 4 via the FAPyG N9 radical. Pathways 1 and 2 are not considered in Wetmore's publication, and the relative energies of the 2,5 FAPyG isomer, the 8-oxyG radical, the hemiaminal, and the FAPyG N7 radical species are not discussed.

Lowest Energy Pathway. Upon the basis of the solution-phase calculations at the IEF-PCM/B3LYP/aug-cc-pVTZ//B3LYP/6-31+G(d) level of theory with the methoxyethyl substituent and the gas-phase calculations at the B3LYP/6-31+G(d) level of theory with three different substituents, the lowest energy mechanism for formation of either 2,5FAPyG or FAPyG appears to be pathway 2, via the 8-oxyG radical. The next most favorable mechanism is pathway 4, ring opening of 8-OHGrad followed by tautomerization. Depending on the reducing agent, pathway 3 is probably less favorable than pathway 4. The closed shell mechanism, pathway 1, has the highest barrier and is the least likely.

In aqueous solution, the relative energy of the ring-opening transition state, **10**-TS, for formation of the 2,5FAPyG isomer via pathway 2 is within 2.8 kcal/mol of the transition state, **13**-TS, for formation of FAPyG. These data suggest that both the 2,5FAPyG and the FAPyG isomers could be formed initially. Furthermore, the 2,5FAPyG isomer can be converted to the FAPyG isomer via the hemiaminal intermediate (**3**). The barrier height for this reverse reaction is estimated to be 23.5 kcal/mol at the IEF-PCM/B3LYP/aug-cc-pVTZ//B3LYP/6-31+G(d) level of theory.

Identification of Guanine Adducts. While the fragmentation patterns between the hemiaminal (**3**), formimidic acid (**19**), and the two formamidopyrimidines (**5** and **7**) will differ slightly, it is unlikely that mass spectral analysis could be used to clearly distinguish between the four guanine adducts. It should, however, be possible to identify the adducts using either NMR spectroscopy or vibrational spectroscopy (IR).

NMR isotropic shielding tensors were calculated for the 2,5FAPyG, FAPyG, hemiaminal, and formimidic acid adducts in the gas phase at the B3LYP/6-31+G(d) level of theory with the hydrogen as the N9 substituent. The predicted differences in the chemical shifts of the 2,5FAPyG, hemiaminal, and formimidic acid adducts are provided in Table 2. Relative to FAPyG, the predicted ^{13}C spectrum of 2,5FAPyG shows a 19

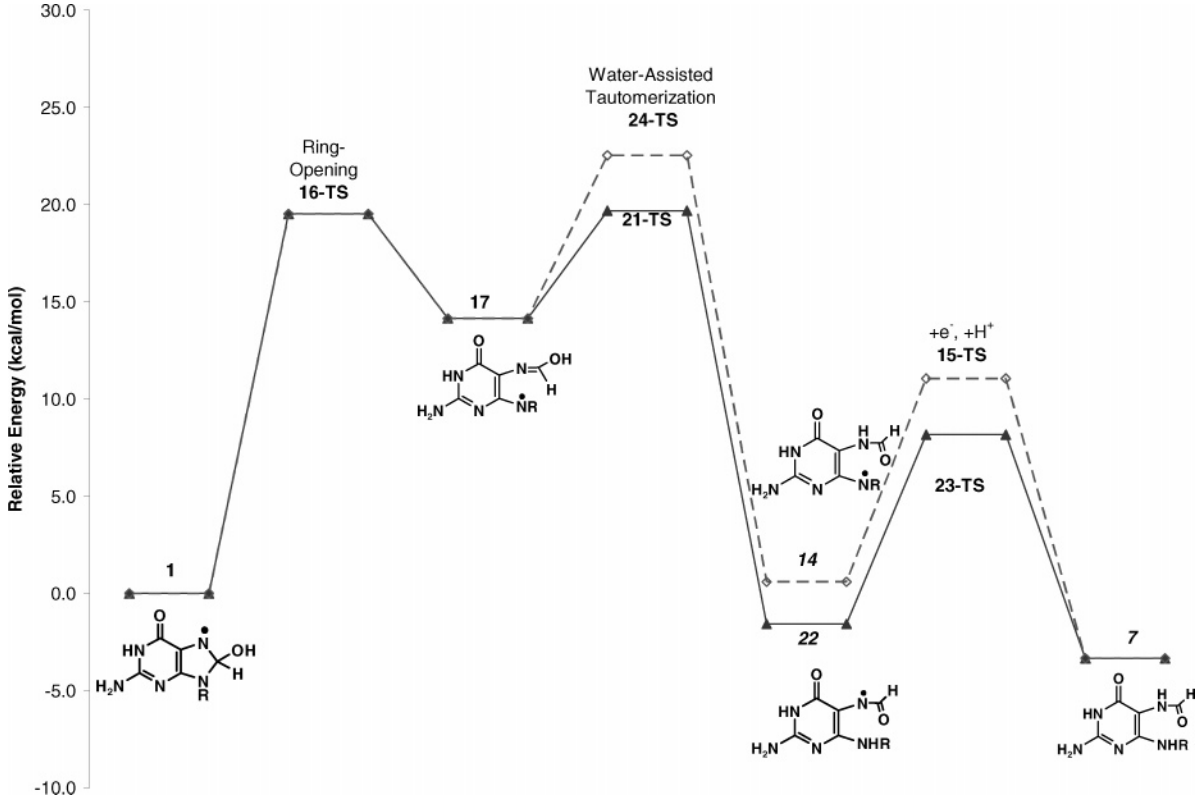

Figure 9. Pathway 4: Relative energy in solution of the open shell (radical) mechanism for ring opening of 8-OHGrad (**1**) to FAPyG (**7**) via the formimidic acid radical (**17**) calculated at IEF-PCM/B3LYP/aug-cc-pVTZ//B3LYP/6-31G(d). The data are for the adducts with methoxyethyl as the N9 substituent. The forward barrier height for ring opening of the 8-OHGrad to the formimidic acid radical is calculated to be 19.5 kcal/mol. Water-assisted tautomerization of the formimidic acid radical to the FAPyG N7 radical (**22**) has a barrier height of 5.6 kcal/mol; tautomerization to the FAPyG N9 radical (**14**) has an estimated forward barrier height of 8.4 kcal/mol.

Table 2. Predicted ^{13}C and ^{15}N Chemical Shifts of the 2,5FAPyG, Hemiaminal, and Formimidic Acid Adducts of Guanine Relative to FAPyG Calculated at B3LYP/6-31+G(d) for the Hydrogen Substituent at N9

Carbon 13 NMR Comparison
(Chemical Shifts Relative to FAPyG in ppm)[a]

carbon no.	FAPyG (**7**)	25FAPyG (**5**)	hemiaminal (**3**)	formimidic acid (**19**)
C2	0	−6.1	1.4	0.8
C4	0	−19.1	−3.4	4.9
C5	0	20.3	4.0	1.6
C6	0	1.2	−7.3	−1.2
C8	0	−2.2	−54.9	−7.5

Nitrogen 15 NMR Comparison
(Chemical Shifts Relative to FAPyG in ppm)[b]

nitrogen no.	FAPyG (**7**)	25FAPyG (**5**)	hemiaminal (**3**)	formimidic acid (**19**)
N1	0	6.4	10.2	6.1
N3	0	5.4	−9.8	−4.6
N7	0	−75.2	−50.5	103.7
N9	0	60.0	15.0	−13.8
NH_2 at C2	0	−3.1	−0.4	0.1

[a] For FAPyG, the calculated chemical shifts in ppm relative to TMS are as follows: 142.6 for C2, 147.5 for C4, 95.6 for C5, 150.6 for C6, and 149.7 for C8. [b] For FAPyG, the calculated chemical shifts in ppm relative to NH_3 are as follows: 143.1 for N1, 191.6 for N3, 132.6 for N7, 94.4 for N9, and 69.4 for the NH_2 group at C2.

ppm increase in shielding (right shift) of the C4 carbon of the pyrimidine ring and a concomitant 20 ppm decrease in shielding (left shift) of the C5 carbon. A similar pattern is predicted for the ^{15}N spectrum, with a 75 ppm increase in shielding for the nitrogen at N7 and a 60 ppm decrease in shielding for the N9 nitrogen of 2,5FAPyG relative to the FAPyG isomer. The hemiaminal should be clearly distinguishable from the two formamidopyrimidine adducts and the formimidic acid, as its predicted ^{13}C NMR spectrum shows a marked increase in shielding (55 ppm) of the carbon at C8 relative to FAPyG. The predicted ^{13}C NMR spectrum of the formimidic acid moiety is very similar to that of FAPyG. This adduct should be distinguishable from the other three compounds via ^{15}N NMR, as there is a 104 ppm increase in chemical shift for the nitrogen at N7 relative to FAPyG indicating marked deshielding. Both the 2,5FAPyG and the hemiaminal adducts have increased shielding of this nitrogen as indicated by the 75 ppm decrease in chemical shift. Several authors have conducted NMR studies on formamidopyrimidine adducts of guanine (*25*, *58*, *59*). Upon the basis of their proton NMR data, two of the authors have suggested that the experimentally determined barrier heights for rotation about the N7−C8 bond in FAPyG is 17.7 kcal/mol (*25*) for interconversion between rotamers 1 and 2 (Figure 3) and 22.9−23.0 kcal/mol (*59*) for interconversion between rotamers 1 and 4. In the latter experiment, FAPyG was substituted at N7 with a methyl group rather than a hydrogen. Humphries et al. (*58*) conducted an ^{15}N NMR on formamidopyrimidine adducts with ^{15}N substitution at the N7 position of the original guanine and found an equal population of two species at 110.6 and 111.7 ppm relative to ammonia. These signals were attributed by the author to two rotamers of the FAPyG isomer. In the same study, ^{1}H NMR data from glutathione-substituted FAPy glycosides indicated that four different conformers were present. Consistent with the FAPyG isomer, all of the spectra showed doublet splitting of the formyl proton signal as would be expected for a geminal to the ^{15}N isotope located at the N7 position.

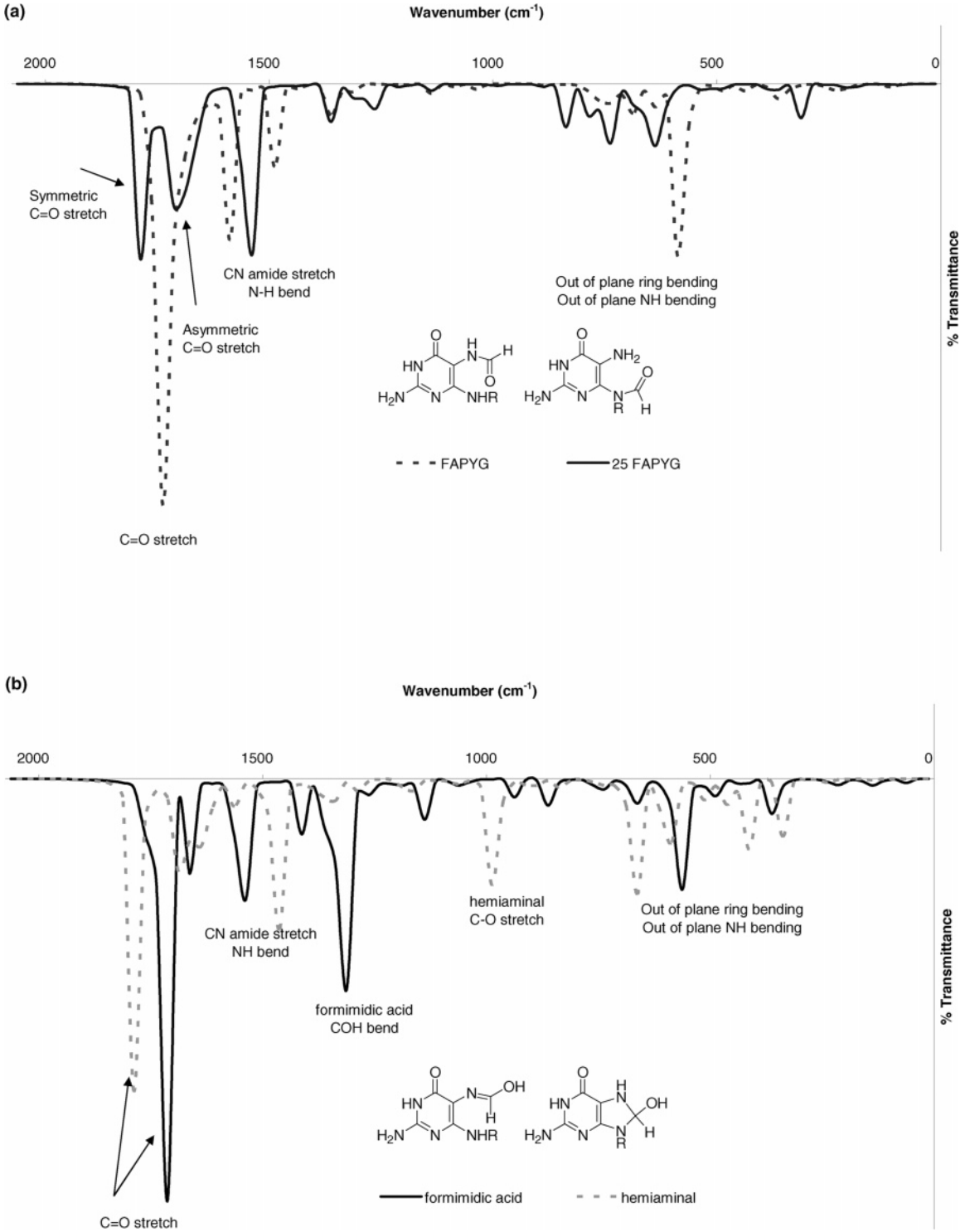

Figure 10. Predicted IR spectra for (a) the 2,5FAPyG (**5**) and FAPyG (**7**) adducts of guanine and (b) the formimidic acid (**19**) and hemiaminal (**3**) adducts of guanine at the B3LYP/6-31+G(d) level of theory. Data are for compounds with hydrogen as the substituent at N9.

The calculated infrared spectra shown in Figure 10 of the 2,5FAPyG, FAPyG, hemiaminal, and formimidic acid adducts differ in the wavenumber regions typical of carbonyl stretching, C−O stretching, and N−H stretching and bending. It should be possible to differentiate experimentally between the various adducts if they can be isolated before conversion to FAPyG. Both 2,5FAPyG and FAPyG have two carbonyl stretching frequencies representing symmetric and asymmetric stretching of the pair of carbonyl groups. For the 2,5FAPyG isomer, the calculations suggest that the intensity of the two frequencies is about equal and that there is about a 28−37 cm^{-1} difference between the two peaks, with the symmetric stretch occurring at around 1760−1770 cm^{-1}. The calculations suggest that the FAPyG isomer has a strong asymmetric carbonyl stretching peak at 1715−1725 cm^{-1} and a weak symmetric stretching peak at 1745−1750 cm^{-1}. The hemiaminal and formimidic acid adducts have only one carbonyl stretching frequency. The carbonyl stretching frequency of the formimidic acid group is lower than that of the hemiaminal perhaps due to conjugation of the carbonyl group with the formimidic acid group. The formimidic acid adduct can be further differentiated from the other adducts as it has a moderately intense and unique C−O−H bending

frequency at about 1280 cm^{-1}. The hemiaminal adduct is predicted to have a moderately intense and unique C−O stretching frequency at about 1000 cm^{-1}.

Conclusions

The potential energy surface for modification of guanine leading to the formation of formamidopyrimidine adducts has been mapped out using DFT for three different substituents at the N9 position of guanine in the gas phase and in aqueous solution for N9-methoxyethyl guanine. With the exception of the 2,5FAPyG and its corresponding radical, the choice of the substituent at the N9 position had little effect on the relative enthalpies of the reactants, intermediates, transition states, and products. Results from a variety of experimental studies indicate that numerous compounds may be formed following addition of a hydroxyl radical to guanine, some of which react over time to form the observed FAPyG adduct. Of the four reaction pathways shown in Scheme 2, pathway 2 appears to be the lowest energy pathway and may be kinetically favored over the other three pathways. The calculations indicate that this mechanism for modification of guanine may yield a 2,5FAPyG adduct, which is thermodynamically less stable than the FAPyG adduct but may be formed at least initially. Interconversion of the two isomers is possible via the hemiaminal adduct. Additional species formed as part of these mechanistic pathways are the formimidic acid and hemiaminal adducts, but these are less stable than FAPyG or 2,5FAPyG. Calculations of the IR and NMR spectra suggest that it will be possible to differentiate between these intermediate adducts.

Acknowledgment. This work was supported by grants from the National Science Foundation (CHE 0512144 to H.B.S. and CHE 0514612 to C.J.B.). We thank C&IT, ISC, and the Department of Chemistry at Wayne State University for computer time.

Supporting Information Available: Molecular geometries in Cartesian coordinates and gas-phase relative enthalpies for all adducts and corresponding transition states. This material is available free of charge via the Internet at http://pubs.acs.org.

References

(1) Steenken, S. (1989) Purine-bases, nucleosides, and nucleotides—Aqueous-solution redox chemistry and transformation reactions of their radical cations and e- and OH adducts. *Chem. Rev. 89*, 503−520.
(2) Breen, A. P., and Murphy, J. A. (1995) Reactions of oxyl radicals with DNA. *Free Radical Biol. Med. 18*, 1033−1077.
(3) Burrows, C. J., and Muller, J. G. (1998) Oxidative nucleobase modifications leading to strand scission. *Chem. Rev. 98*, 1109−1151.
(4) Candeias, L. P., and Steenken, S. (2000) Reaction of HO• with guanine derivatives in aqueous solution: Formation of two different redox-active OH-adduct radicals and their unimolecular transformation reactions. Properties of G(-H)(center dot). *Chem. Eur. J. 6*, 475−484.
(5) Evans, M. D., Dizdaroglu, M., and Cooke, M. S. (2004) Oxidative DNA damage and disease: Induction, repair and significance. *Mutat. Res.—Rev. Mutat. Res. 567*, 1−61.
(6) Kalam, M. A., Haraguchi, K., Chandani, S., Loechler, E. L., Moriya, M., Greenberg, M. M., and Basu, A. K. (2006) Genetic effects of oxidative DNA damages: Comparative mutagenesis of the imidazole ring-opened formamidopyrimidines (FAPy lesions) and 8-oxo-purines in simian kidney cells. *Nucleic Acids Res. 34*, 2305−2315.
(7) Birincioglu, M., Jaruga, P., Chowdhury, G., Rodriguez, H., Dizdaroglu, M., and Gates, K. S. (2003) DNA base damage by the antitumor agent 3-amino-1,2,4-benzotriazine 1,4-dioxide (tirapazamine). *J. Am. Chem. Soc. 125*, 11607−11615.
(8) Neeley, W. L., and Essigmann, J. M. (2006) Mechanisms of formation, genotoxicity, and mutation of guanine oxidation products. *Chem. Res. Toxicol. 19*, 491−505.
(9) Lindahl, T. (1993) Instability and decay of the primary structure of DNA. *Nature 362*, 709−715.
(10) Smith, K. C. (1992) Spontaneous mutagenesis—Experimental, genetic and other factors. *Mutat. Res. 277*, 139−162.
(11) Wetmore, S. D., Boyd, R. J., and Eriksson, L. A. (2000) Electron affinities and ionization potentials of nucleotide bases. *Chem. Phys. Lett. 322*, 129−135.
(12) Kasai, H., Yamaizumi, Z., Berger, M., and Cadet, J. (1992) Photosensitized formation of 7,8-dihydro-8-oxo-2′-deoxyguanosine (8-hydroxy-2′-deoxyguanosine) in DNA by riboflavin—A nonsinglet oxygen mediated reaction. *J. Am. Chem. Soc. 114*, 9692−9694.
(13) Cullis, P. M., Malone, M. E., and Merson Davies, L. A. (1996) Guanine radical cations are precursors of 7,8-dihydro-8-oxo-2′-deoxyguanosine but are not precursors of immediate strand breaks in DNA. *J. Am. Chem. Soc. 118*, 2775−2781.
(14) Crean, C., Geacintov, N. E., and Shafirovich, V. (2005) Oxidation of guanine and 8-oxo-7,8-dihydroguanine by carbonate radical anions: Insight from oxygen-18 labeling experiments. *Angew. Chem., Int. Ed. 44*, 5057−5060.
(15) Misiaszek, R., Crean, C., Joffe, A., Geacintov, N. E., and Shafirovich, V. (2004) Oxidative DNA damage associated with combination of guanine and superoxide radicals and repair mechanisms via radical trapping. *J. Biol. Chem. 279*, 32106−32115.
(16) Shukla, L. I., Adhikary, A., Pazdro, R., Becker, D., and Sevilla, M. D. (2004) Formation of 8-oxo-7,8-dihydroguanine-radicals in gamma-irradiated DNA by multiple one-electron oxidations. *Nucleic Acids Res. 32*, 6565−6574.
(17) Berger, M., and Cadet, J. (1985) Isolation and characterization of the radiation-induced degradation products of 2′-deoxyguanosine in oxygen-free aqueous-solutions. *Z. Naturforsch., B: Chem. Sci. 40*, 1519−1531.
(18) Raoul, S., Bardet, M., and Cadet, J. (1995) Gamma-irradiation of 2′-deoxyadenosine in oxygen-free aqueous-solutions—Identification and conformational features of formamidopyrimidine nucleoside derivatives. *Chem. Res. Toxicol. 8*, 924−933.
(19) Van Hemmen, J. J., and Bleichrodt, J. F. (1971) The decomposition of adenine by ionizing radiation. *Radiat. Res. 46*, 444−456.
(20) Jiang, Y. L., Wiederholt, C. J., Patro, J. N., Haraguchi, K., and Greenberg, M. M. (2005) Synthesis of oligonucleotides containing FAPy• dG (N-6-(2-deoxy-α,β-D-erythropentofuranosyl)-2,6-diamino-4-hydroxy- 5-formamidopyrimidine) using a 5′-dimethoxytrityl dinucleotide phosphoramidite. *J. Org. Chem. 70*, 141−149.
(21) Ober, M., Hsu, G. W., Beese, L. S., Coste, F., Boiteux, S., Zelwer, C., Castaing, B., and Carell, T. (2005) Replication and repair of the oxidative DNA lesions 8-oxoG and FAPyG. *ACS Abstr. Pap. 229*, U260−U260.
(22) Ober, M., Muller, H., Pieck, C., Gierlich, J., and Carell, T. (2005) Base pairing and replicative processing of the formamidopyrimidine-dG DNA lesion. *J. Am. Chem. Soc. 127*, 18143−18149.
(23) Crespo-Hernandez, C. E., and Arce, R. (2004) Formamidopyrimidines as major products in the low- and high-intensity UV irradiation of guanine derivatives. *J. Photochem. Photobiol., B 73*, 167−175.
(24) Coste, F., Ober, M., Carell, T., Boiteux, S., Zelwer, C., and Castaing, B. (2004) Structural basis for the recognition of the FAPydG lesion (2,6-diamino-4-hydroxy-5-formamidopyrimidine) by formamidopyrimidine-DNA glycosylase. *J. Biol. Chem. 279*, 44074−44083.
(25) Burgdorf, L. T., and Carell, T. (2002) Synthesis, stability, and conformation of the formamidopyrimidine G DNA lesion. *Chem. Eur. J. 8*, 293−301.
(26) Reynisson, H., and Steenken, S. (2002) DFT calculations on the electrophilic reaction with water of the guanine and adenine radical cations. A model for the situation in DNA. *Phys. Chem. Chem. Phys. 4*, 527−532.
(27) Llano, J., and Eriksson, L. A. (2004) Oxidation pathways of adenine and guanine in aqueous solution from first principles electrochemistry. *Phys. Chem. Chem. Phys. 6*, 4707−4713.
(28) Jena, N. R., and Mishra, P. C. (2005) Mechanisms of formation of 8-oxoguanine due to reactions of one and two OH center dot radicals and the H2O2 molecule with guanine: A quantum computational study. *J. Phys. Chem. B 109*, 14205−14218.
(29) Wetmore, S. D., Boyd, R. J., and Eriksson, L. A. (1998) Comparison of experimental and calculated hyperfine coupling constants. Which radicals are formed in irradiated guanine? *J. Phys. Chem. B 102*, 9332−9343.
(30) O'Neill, P. (1983) Pulse radiolytic study of the interaction of thiols and ascorbate with OH adducts of Dgmp and Dg—Implications for DNA-repair processes. *Radiat. Res. 96*, 198−210.
(31) O'Neill, P., and Chapman, P. W. (1985) Potential repair of free-radical adducts of Dgmp and Dg by a series of reductants—A pulse radiolytic study. *Int. J. Radiat. Biol. 47*, 71−80.
(32) Wetmore, S. D., Boyd, R. J., LLano, J., Lundqvist, M. J., and Eriksson, L. A. (2000) Hydroxyl radical reactions in biological media. In *Recent Advances in Density Functional Methods* (Barone, V., Bencini, A., Fantucci, P., Eds.) Vol. 3, pp 387−415, World Scientific, Singapore.

(33) Frisch, M. J., Trucks, G. W., Schlegel, H. B., Scuseria, G. E., Robb, M. A., Cheeseman, J. R., Montgomery, J. A., Jr., Vreven, T., Scalmani, G., Kudin, K. N., Iyengar, S. S., Tomasi, J., Barone, V., Mennucci, B., Cossi, M., Rega, N., Petersson, G. A., Nakatsuji, H., Hada, M., Ehara, M., Toyota, K., Fukuda, R., Hasegawa, J., Ishida, M., Nakajima, T., Honda, Y., Kitao, O., Nakai, H., Li, X., Hratchian, H. P., Peralta, J. E., Izmaylov, A. F., Brothers, E., Staroverov, V., Kobayashi, R., Normand, J., Burant, J. C., Millam, J. M., Klene, M., Knox, J. E., Cross, J. B., Bakken, V., Adamo, C., Jaramillo, J., Gomperts, R., Stratmann, R. E., Yazyev, O., Austin, A. J., Cammi, R., Pomelli, C., Ochterski, J. W., Ayala, P. Y., Morokuma, K., Voth, G. A., Salvador, P., Dannenberg, J. J., Zakrzewski, V. G., Dapprich, S., Daniels, A. D., Strain, M. C., Farkas, O., Malick, D. K., Rabuck, A. D., Raghavachari, K., Foresman, J. B., Ortiz, J. V., Cui, Q., Baboul, A. G., Clifford, S., Cioslowski, J., Stefanov, B. B., Liu, G., Liashenko, A., Piskorz, P., Komaromi, I., Martin, R. L., Fox, D. J., Keith, T., Al-Laham, M. A., Peng, C. Y., Nanayakkara, A., Challacombe, M., Chen, W., Wong, M. W., and Pople, J. A. (2006) *Gaussian DV*, Gaussian, Inc., Wallingford, CT.

(34) Becke, A. D. (1993) Density functional theory. III. The role of exact exchange. *J. Chem. Phys. 98*, 5648−5652.

(35) Becke, A. D. (1988) Density functional exchange energy approximation with correct asymptotic behavior. *Phys. Rev. A 38*, 3098−3100.

(36) Lee, C., Yang, W., and Parr, R. D. (1988) Development of the Colle-Salvetti correlation energy formula into a functional of the electron density. *Phys. Rev. B 37*, 785−789.

(37) Ditchfield, R., Hehre, W. J., and Pople, J. A. (1971) Self-consistent molecular-orbital methods. IX. An extended Gaussian-type basis for molecular-orbital studies of organic molecules. *J. Chem. Phys. 54*, 724−728.

(38) Hehre, W. J., Ditchfield, R., and Pople, J. A. (1972) Self-consistent molecular orbital methods. XII. Further extensions of Gaussian-type basis sets for use in molecular Orbital studies of organic molecules. *J. Chem. Phys. 56*, 2257−2261.

(39) Hariharan, P. C., and Pople, J. A. (1973) The influence of polarization functions on molecular orbital hydrogenation energies. *Theor. Chim. Acta 28*, 213−222.

(40) Hariharan, P. C., and Pople, J. A. (1974) Accuracy of AH, equilibrium geometries by single determinant molecular orbital theory. *Mol. Phys. 27*, 209−214.

(41) Gordon, M. S. (1980) The isomers of silacyclopropane. *Chem. Phys. Lett. 76*, 163−168.

(42) Francl, M. M., Pietro, W. J., Hehre, W. J., Binkley, J. S., Gordon, M. S., Defrees, D. J., and Pople, J. A. (1982) Self-consistent molecular-orbital methods. 23. A polarization-type basis set for 2nd-row elements. *J. Chem. Phys. 77*, 3654−3665.

(43) Cances, E., Mennucci, B., and Tomasi, J. (1997) A new integral equation formalism for the polarizable continuum model: Theoretical background and applications to isotropic and anisotropic dielectrics. *J. Chem. Phys. 107*, 3032−3041.

(44) Mennucci, B., and Tomasi, J. (1997) Continuum solvation models: A new approach to the problem of solute's charge distribution and cavity boundaries. *J. Chem. Phys. 106*, 5151−5158.

(45) Mennucci, B., Cances, E., and Tomasi, J. (1997) Evaluation of solvent effects in isotropic and anisotropic dielectrics and in ionic solutions with a unified integral equation method: Theoretical bases, computational implementation, and numerical applications. *J. Phys. Chem. B 101*, 10506−10517.

(46) Tomasi, J., Mennucci, B., and Cances, E. (1999) The IEF version of the PCM solvation method: An overview of a new method addressed to study molecular solutes at the QM ab initio level. *J. Mol. Struct. (Theochem) 464*, 211−226.

(47) Chipman, D. M. (2000) Reaction field treatment of charge penetration. *J. Chem. Phys. 112*, 5558−5565.

(48) Cances, E., and Mennucci, B. (2001) Comment on Reaction field treatment of charge penetration. *J. Chem. Phys. 114*, 4744−4745.

(49) Kendall, R. A., Dunning, T. H., and Harrison, R. J. (1992) Electron-affinities of the 1st-row atoms revisited−Systematic basis-sets and wave-functions. *J. Chem. Phys. 96*, 6796−6806.

(50) Oikawa, S., Hiraku, Y., Fujiwara, T., Saito, I., and Kawanishi, S. (2002) Site-specific hydroxylation at polyguanosine in double-stranded DNA by nickel(II) in the presence of SH compounds: Comparison with singlet oxygen-induced DNA damage. *Chem. Res. Toxicol. 15*, 1017−1022.

(51) Lamoureux, G. V., and Whitesides, G. M. (1993) Synthesis of dithiols as reducing agents for disulfides in neutral aqueous-solution and comparison of reduction potentials. *J. Org. Chem. 58*, 633−641.

(52) Scott, A. P., and Radom, L. (1996) Harmonic vibrational frequencies: An evaluation of Hartree−Fock, Moller−Plesset, quadratic configuration interaction, density functional theory, and semiempirical scale factors. *J. Phys. Chem. 100*, 16502−16513.

(53) McQuarrie, D. A. (1973) *Statistical Thermodynamics*, University Science Books, Mill Valley, CA.

(54) Adamo, C., and Barone, V. (1998) Toward chemical accuracy in the computation of NMR shieldings: The PBE0 model. *Chem. Phys. Lett. 298*, 113−119.

(55) Baldridge, K. K., and Siegel, J. S. (1999) Correlation of empirical delta(TMS) and absolute NMR chemical shifts predicted by ab initio computations. *J. Phys. Chem. A 103*, 4038−4042.

(56) Giesen, D. J., and Zumbulyadis, N. (2002) A hybrid quantum mechanical and empirical model for the prediction of isotropic C-13 shielding constants of organic molecules. *Phys. Chem. Chem. Phys. 4*, 5498−5507.

(57) Ravanat, J. L., Martinez, G. R., Medeiros, M. H. G., Di Mascio, P., and Cadet, J. (2004) Mechanistic aspects of the oxidation of DNA constituents mediated by singlet molecular oxygen. *Arch. Biochem. Biophys. 423*, 23−30.

(58) Humphreys, W. G., and Guengerich, F. P. (1991) Structure of formamidopyrimidine adducts as determined by NMR using specifically N-15-labeled guanosine. *Chem. Res. Toxicol. 4*, 632−636.

(59) Boiteux, S., Belleney, J., Roques, B. P., and Laval, J. (1984) Two rotameric forms of open ring 7-methylguanine are present in alkylated polynucleotides. *Nucleic Acids Res. 12*, 5429−5439.

TX060187T